

Wright State University

CORE Scholar

---

[Browse all Theses and Dissertations](#)

[Theses and Dissertations](#)

---

2018

## Determination Of Dose Effects When Including Attenuation Of The Treatment Table Into Treatment Planning Computer Modeling

Abdullah Alshamrany  
*Wright State University*

Follow this and additional works at: [https://corescholar.libraries.wright.edu/etd\\_all](https://corescholar.libraries.wright.edu/etd_all)



Part of the [Physics Commons](#)

---

### Repository Citation

Alshamrany, Abdullah, "Determination Of Dose Effects When Including Attenuation Of The Treatment Table Into Treatment Planning Computer Modeling" (2018). *Browse all Theses and Dissertations*. 1916. [https://corescholar.libraries.wright.edu/etd\\_all/1916](https://corescholar.libraries.wright.edu/etd_all/1916)

This Thesis is brought to you for free and open access by the Theses and Dissertations at CORE Scholar. It has been accepted for inclusion in Browse all Theses and Dissertations by an authorized administrator of CORE Scholar. For more information, please contact [library-corescholar@wright.edu](mailto:library-corescholar@wright.edu).

**Determination Of Dose Effects When Including Attenuation Of The Treatment  
Table Into Treatment Planning Computer Modeling**

A thesis submitted in partial fulfillment  
of the requirements for the degree of  
Master of Science

By

ABDULLAH ALSHAMRANY  
B.S., King Saud University, 2011

2018  
Wright State University

WRIGHT STATE UNIVERSITY

GRADUATE SCHOOL

December 7, 2017

I HEREBY RECOMMEND THAT THE THESIS PREPARED UNDER MY  
SUPERVISION BY Abdullah Alshamrany ENTITLED Determination of Dose Effects  
when Including Attenuation of the Treatment Table into Treatment Planning Computer  
Modeling BE ACCEPTED IN PARTIAL FULFILLMENT OF THE REQUIREMENTS  
FOR THE DEGREE OF Master of Science.

---

Brent D. Foy, Ph.D.  
Thesis Director

---

Jason A. Deibel, Ph.D.  
Chair, Department of Physics

Committee on  
Final Examination

---

Brent D. Foy, Ph.D.  
Thesis Director

---

Michael Gossman, M.S., DABR, FAAPM

---

Amit R. Sharma, Ph.D.

---

Barry Milligan, Ph.D.  
Interim Dean of the Graduate School

## ABSTRACT

Alshamrany, Abdullah. M.S. Department of Physics, Wright State University, 2018.  
Determination of Dose Effects when Including Attenuation of the Treatment Table into  
Treatment Planning Computer Modeling.

During radiation treatment, the patient commonly lies on a horizontal treatment table called a couch. The material used for the couch is chosen during the manufacturing process so as to minimize the effect of the couch on dose delivery, but it still has an effect. In addition to couch attenuation on the beam, the modern approach of using multiple beam angles for dose delivery makes treatment planning in the presence of the couch more challenging. However, the effect of the couch is not always considered when creating treatment plans, generally due to treatment planning software limitations. In this evaluation, the effects of the Varian Medical Systems, Inc® (Palo Alto, CA) Model IGRT Couch Top® on the dose distribution of head and neck cancer treatment was determined for a linear accelerator operating at 6 MV. Four head and neck cancer patients were selected for the study. Varian Model Eclipse® treatment planning software was used to create two Volumetric Modulated Arc Therapy (VMAT) plans. One plan assumed the couch was not present, and one assumed it was present. Both plans were optimized to achieve the same physician directed dose objectives. Comparisons were then made using the planning system's Dose Volume Histogram (DVH) statistical and volumetric data. Dose changes to the tumor volumes along with normal tissue structures around the target area were clinically assessed. The mean dose to the tumor

was reduced by 0.5 to 0.65 Gy as a consequence of including the couch during planning.

Doses to surrounding normal tissues showed variable, yet significant effects.

## TABLE OF CONTENTS

<b><u>Section</u></b>	<b><u>Page</u></b>
<b>1.0 INTRODUCTION.....</b>	<b>1</b>
<b>2.0 Background and Theory .....</b>	<b>4</b>
2.1 External Beam Radiation Therapy .....	4
2.2 Interaction of Photons with Matter .....	5
2.3 Absorbed Dose.....	7
2.4 Dose Distribution .....	8
2.5 Hounsfield Unit.....	10
2.6 Target Volumes.....	10
2.7 Current Treatment Modalities .....	11
<b>3.0. METHODS AND MATERIALS .....</b>	<b>13</b>
3.1 Planning .....	13
3.2 Procedure .....	14
3.2.1 Patient Selection and the Cases Descriptions .....	14
3.2.2 Treatment Plan Set up.....	14
3.2.2.1 Contouring both Target Structures and OARs.....	15
3.2.2.2 Dose Constraints for Target Structures and OARs .....	17
3.2.2.3 Inserting the IGRT Couch Top® on the Couch Excluded Plans .....	18

## TABLE OF CONTENTS (CONTINUED)

<b><u>Section</u></b>	<b><u>Page</u></b>
3.3 Dose Distribution Analysis .....	20
3.4 Beam Attenuation Measurement.....	22
3.5 Theoretical Calculations of Couch Attenuation and HU .....	23
<b>4.0. RESULTS</b> .....	25
4.1 Results of Beam Attenuation Measurements .....	25
4.2 Result of Theoretical Calculations of Couch Attenuation and HU.....	25
4.3 Patient Results.....	25
4.3.1 First Patient .....	25
4.3.2 Second Patient.....	30
4.3.3 Third Patient.....	34
4.3.4 Fourth Patient.....	38
4.4 Summary of Dose Differences between Two Plans for All Patients .....	44
<b>5.0 DISCUSSION</b> .....	45
5.1 Target Structures .....	45
5.2 Normal Structures .....	46
5.2.1 Spinal Cord .....	46
5.2.3 Mandible .....	46
5.2.4 Larynx .....	46
5.2.5 Right and Left Parotid Gland.....	47
<b>CONCLUSION</b> .....	48
<b>REFERENCES</b> .....	49

## LIST OF FIGURES

<b><u>Figure</u></b>	<b><u>Page</u></b>
Figure 1: Schematic of a Linear Accelerator .....	5
Figure 2: Schematic plot of absorbed dose and kerma as functions of depth.....	9
Figure 3: Central axis depth dose distribution for different quality photon beam.....	9
Figure 4: Dynamic multileaf collimators .....	11
Figure 5: CT image of the tongue base with target structures .....	16
Figure 6: CT image of the tongue base case with normal organs .....	16
Figure 7: The Varian <sup>®</sup> IGRT Couch Top <sup>®</sup> .....	18
Figure 8: The IGRT couch model in Eclipse .....	19
Figure 9: Dose Volume Histogram (DVH).....	21
Figure 10: Measurement setup for couchtopy beam attenuation .....	23
Figure 11: Does percentage distribution for mandible between 85% and 35% of the volume.....	28
Figure 12: Does percentage distribution for oral cavity between 75% and 5% of the volume.....	29
Figure 13: Does percentage distribution for spinal cord between 75% and 5% of the volume.....	29



## LIST OF FIGURES (CONTINUED)

<b><u>Figure</u></b>	<b><u>Page</u></b>
Figure 14: Does percentage distribution for larynx between 95% and 5% of the Volume.....	30
Figure 15: Does percentage distribution for mandible between 60% and 5% of the volume.....	32
Figure 16: Does percentage distribution for spinal cord between 40% and 5% of the volume.....	33
Figure 17: Does percentage distribution for right parotid gland between 90% and 10% of the volume.....	36
Figure 18: Does percentage distribution for spinal cord between 75% and 10% of the volume.....	37
Figure 19: Does percentage distribution for larynx .....	37
Figure 20: Does percentage distribution for right brachial plexus between 90% and 40% of the volume .....	38
Figure 21: Does percentage distribution for spinal cord between 70% and 10% of the volume.....	41
Figure 22: Does percentage distribution for larynx between 95% and 15% of the Volume.....	41
Figure 23: Does percentage distribution for left parotid gland between 75% and 5% of the volume.....	42

**LIST OF FIGURES (CONTINUED)**

<b><u>Figure</u></b>	<b><u>Page</u></b>
Figure 24: Does percentage distribution for right brachial plexus between 90% and 65% of the volume .....	43
Figure 25: Does percentage distribution for left brachial plexus between 90% and 20% of the volume.....	43

## LIST OF TABLES

<b><u>Table</u></b>	<b><u>Page</u></b>
Table 1: Target structures dose constraints.....	17
Table 2: OARs dose constraints.....	17
Table 3: Beam attenuation of IGRT couch at different angles .....	25
Table 4: First patient DVH analysis for the targets structures.....	26
Table 5: Homogeneity Index (HI) of PTV 70 for the first patient.....	26
Table 6: First patient DVH analysis for some organs at risk .....	27
Table 7: Second patient DVH analysis for the targets structures .....	31
Table 8: Homogeneity Index (HI) of PTV 70 for the second patient .....	31
Table 9: Second patient DVH analysis for some organs at risk .....	32
Table 10: Third patient DVH analysis for the targets structures .....	34
Table 11: Homogeneity Index (HI) of PTV 70 for the third patient.....	34
Table 12: Third patient DVH analysis for some organs at risk .....	35
Table 13: Fourth patient DVH analysis for the targets structures .....	39
Table 14: Homogeneity Index (HI) of PTV 70 for the fourth patient .....	39
Table 15: Fourth patient DVH analysis for some organs at risk.....	40
Table 16: Mean dose change in the target Structures for the all patients [% of 70 Gy] ....	44
Table 17: Mean dose changes for some normal structures [% of 70 Gy].....	44

## 1. INTRODUCTION

In current external beam radiotherapy such as intensity modulated radiotherapy (IMRT) and volumetric modulated arc therapy (VMAT), patients should receive the prescribed dose with higher accuracy than for ordinary three-dimensional conformal radiation therapy (3DCRT). In all of these treatment techniques, the treatment fields are routinely required to penetrate the treatment couch. In the past, medical physicists have not considered the couch during the computerized treatment planning process due to complexities in modeling the device with high accuracy. This remains common practice for most institutions even if the table is made of low-density carbon fiber.<sup>1,2</sup> Studies have shown that a variety of currently marketed couch tops produce significant beam attenuation. McCormack has found that a 6 MV photon beam is attenuated by 2% at 0° angle and a remarkable 9% at 70° angle respect to posterior beam normal incidence.<sup>3</sup> Njeh has measured the attenuation of the carbon fiber couch for the case of intensity-modulated radiation therapy fields and has found a couch attenuation as high as 10% at 6 MV.<sup>4</sup> Moreover, Seppälä has studied the impact of eight couchtops on 6 MV photon beam, and found that the maximum attenuation of 10.8% at an angle of 110°.<sup>5</sup> The Varian® Exact couch effect on 6 MV photon beam has been studied by Veira, *et al* and showed attenuation of up to 15% for oblique beams passing through the couch.<sup>6</sup>

The Varian® IGRT Couch Top® has also been investigated for attenuation by Munjal *et al* and showed a maximum attenuation of 4.8%.<sup>7</sup>

Even though treatment couches are identified to cause beam attenuation, studies about the effect of considering the couch during creation of the treatment plan are insufficient, especially with regards to how attenuation due to the couch plays a role in altering dose-volume histogram (DVH) data.<sup>8</sup> Practical methods are needed to model the couchtops on the patient's treatment plan. In an attempt to advance the science, studies by Myint, Zhihui, and Gerig have evaluated a method for adding treatment couch structures into treatment planning system (TPS) by copying computed tomography (CT) images of couches and then inserting this structure into their TPS.<sup>9,10,11</sup> Mihaylov added an ExacTrac® couch into the Pinnacle® treatment planning system by manually contouring the location and shape of the couch on CT scan data, then assigning Hounsfield units to it that relate to physical density.<sup>12</sup> All the studies found that the agreement between the measured and predicated attenuation in phantom is within 1.4-2% with phantom measurements. However, none of these studies involved actual patient cases for investigating the impact of treatment couches on dose distributions.

A study, evaluating the impact of a Varian® IGRT Couch Top® in the management of prostate treatments via Varian RapidArc® was published by Vanetti, showing the mean dose differences to the target and normal structures between plans with and without Varian® IGRT Couch Top®. For a 6 MV photon beam energy, the mean dose to the prostate gland dropped by 1.3 Gy over the entire course of treatment.<sup>13</sup> This study is not directly applicable to the current study for three reasons. First, the prostate is localized, while head and neck tumors are distributed in a non-uniform fashion through the body.

Second, the couch is thicker in the region needed for prostate treatment than for head and neck treatment. Finally, the surrounding healthy organs are in different locations and have different dose constraints than for head and neck tumors. In this study, the effect of including the couch during treatment planning on doses to tumor targets and surrounding tissues will be investigated, focusing on head and neck tumors. The treatment plans all use the VMAT technique and the Varian TrueBeam® particle accelerator, and the couch under consideration is the Varian® IGRT couch exclusively.

## **2.0 Background and Theory**

### **2.1 External Beam Radiation Therapy**

A linear accelerator is a device used to perform external beam radiation therapy by producing a focused beam of x-ray that can be aimed to patients. Radiation generation all starts with a heated cathode tube, where electrons are boiled off. Those electrons are pulled into a linear tube using an array of quadrupoles that constitute a magnetic field. Along with those magnets, an RF waveguide additionally directs a high frequency wave for further acceleration. Energy increases of upwards to 150 keV/cm are possible using these means. A series of alpha magnets in the gantry bend the electron beam upward and then down, where the patient is to be treated. It is here that the beam can be directed out for direct electron irradiation, or alternatively collide with a target to yield bremsstrahlung x-rays when photon radiation is needed.<sup>14</sup> This x-ray is first collimated by a fixed primary collimator, found immediately below the x-ray target.<sup>14</sup> A flattening filter made of lead or tungsten is used to make the round profile of the x-ray beam more uniform before it passes through a secondary set of collimators.<sup>14</sup> The secondary collimators consist of two movable pairs of lead or tungsten jaws which allow forming a rectangular opening field.<sup>14</sup>

Linear accelerators have a gantry that allows the source to rotate 360° about a horizontal axis. The point of intersection of the gantry axis rotation and the collimator axis (central axis of the beam) is defined as the isocenter (Figure 1).<sup>15</sup>

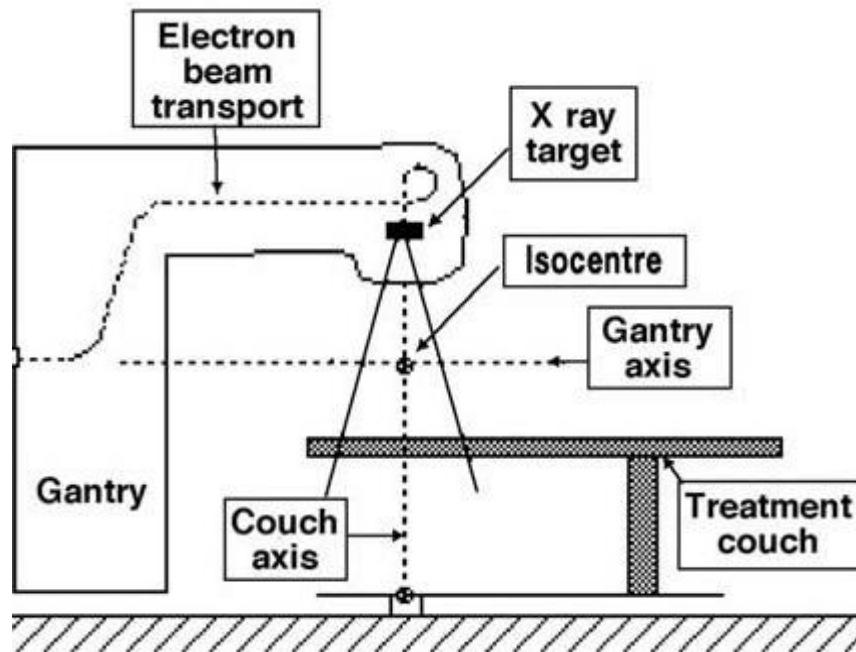


Figure 1: Schematic of a linear accelerator.

(Source: E. B. Podgorsak and J. H. Hendry, Radiation Oncology Physics: A Handbook for Teachers and Students (International Atomic Energy Association, Vienna, 2005))

This rotation allows the treatment beam to enter patients at a defined angle of incidence. While the gantry can move rotationally, the radius of rotation cannot be changed. The distance between the beam source and patients can be controlled by six degree of freedom movement of the treatment couch along pitch, roll, yaw, longitudinal, lateral, and vertical axes.<sup>15</sup>

## 2.2 Interaction of Photons with Matter

When traversing matter, photons will penetrate without interaction, scatter, or be absorbed. The photon interactions are primarily photoelectric effect, Compton scattering, and pair production.<sup>16</sup>

Photoelectric effects take place when low energy photons interact with high atomic number materials.<sup>16</sup> In this phenomenon the photon interacts with an atom and removes



one of the orbital electrons. The photoelectric process predominates when both the energy of incident photon and the electron binding energy are in the same range.<sup>14</sup> The kinetic energy of the ejected photoelectron is equal to the difference between the incident photon energy and electron binding energy.<sup>14,16</sup> Compton scattering occurs when high energy incident photon interacts with outer shell electrons. In this process, the electron receives some energy from the incident photon. The ejected electron and the recoiling photon are emitted with some reduction in energy relative to the incident photon. Pair production can only occur when the energy of the incident photon exceeds 1.02 MeV.<sup>16</sup> In this process, the photon energy is converted due to the electromagnetic field of the atom nucleus and producing a pair consisting of electron and positron. The probability of this interaction increases rapidly with atomic number.<sup>14</sup>

The interaction mechanisms in varying degree cause the photon beam attenuation.<sup>16</sup> The beam attenuation is defined as the reduction of the photon number as it passes through matter. Mathematically,

$$I(x) = I_0 e^{-\mu x}$$

where  $I(x)$  is the intensity transmitted by a thickness  $x$  of the material,  $I_0$  is the incident photon intensity, and  $\mu$  is the attenuation coefficient.<sup>14</sup> For a narrow monoenergetic photon beam the relationship between the transmitted intensity and the absorber thickness is exponential. However, an actual beam used in radiation therapy consists of a spectrum of photon energies. Therefore, the attenuation is not well defined for any specific energy, albeit does follow exponential interaction probabilities. As the absorber thickness increases, the average energy of the transmitted polyenergetic photon beam increases (the

beam becomes harder). Since lower energy photons have a larger coefficient of attenuation than higher energy photons, lower energy photons attenuate quicker.

These x-ray processes are not directly ionizing. All of the primary photon interactions with matter produce fast moving charged particles, electrons, in the medium. These electrons interact with and transfer energy to surrounding particles.<sup>14</sup> For megavoltage radiotherapy, the energy of the incident photons reaching the patient's surface is of the order of 4-25 MV.<sup>14</sup> These high energy photons interact with relatively low effective atomic number of tissue by Compton scattering.<sup>17</sup> After the interaction, the photon is scattered at a relatively small angle yet still moves in a more forward direction. Abiding by the laws of conservation of energy and momentum, the ejected electron also moves in a more forward direction. Remaining energy subtended in the interaction is absorbed by the medium causing the scattering event.<sup>18</sup>

### **2.3 Absorbed Dose**

It is a value quantifies the amount of electron released energies that absorbed by a unit mass of matter. The old unit for absorbed dose is the rad (radiation absorbed dose) which represents 100 ergs imparted to gram of matter.<sup>14</sup>

$$1 \text{ rad} = 100 \text{ ergs/g} = 10^{-2} \text{ J/kg}$$

The SI unit for the absorbed dose is the gray which represents the absorption of 1 joule of energy per kilogram of matter.

$$1 \text{ Gy} = 1 \text{ J/kg}$$

## 2.4 Dose Distribution

As a photon beam travels through a medium, it causes the release of electrons. By contrast, an electron beam can simply be absorbed, causing an absorbed dose. An x-ray beam must first ionize the medium, causing those electrons to be absorbed, causing an absorbed dose.

For megavoltage beams, the maximum dose,  $D_{\max}$ , is located at a depth called maximum depth,  $d_{\max}$ , beyond the patients' surface. The distance between the patient's surface and the  $d_{\max}$  is known as the dose build up region.<sup>14</sup> As the high energy photon beam enters the surface, high speed electrons are released.<sup>14</sup> These high-speed electrons deposit their energy to a distance away from the surface, where the ejected electron reaches its range. The range is the distance traveled before interacting so many times that it has very little energy left, therefore becoming completely absorbed.<sup>14</sup> Since the dose is delivered by the electrons, the dose increases with depth until it reaches a maximum. Also, as the production of the electrons depends on the intensity and the energy of the incident photon beam, the number of electrons produced decreases as the photon beam intensity and energy decrease further in the medium.<sup>14</sup> This reduction in the photon beam energy correlates with the kinetic energy released in the medium (kerma) Figure 2.<sup>14</sup>

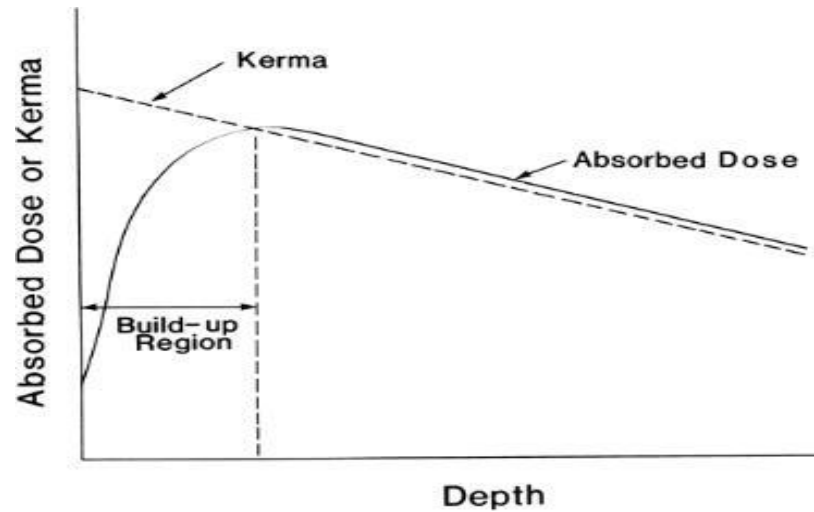


Figure 2: Schematic plot of absorbed dose and kerma as functions of depth. (Source: *The Physics of Radiation Therapy* (p. 164), by F. M. Khan, 2003, Philadelphia, PA: Wolters Company. Copyright 2003 by Lippincott Williams and Wilkins.)

The central axis dose distribution through a medium can be characterized using a Percent Depth Dose (PDD) curve. The PDD is defined as the ratio of the absorbed dose at any depth ( $d$ ) to the maximum absorbed dose at  $d_{\max}$ . As the photon beam energy increases, the  $d_{\max}$  in the phantom or other materials increases, and thus the PDD increases comparatively for depths beyond  $d_{\max}$  Figure 3.<sup>14</sup>

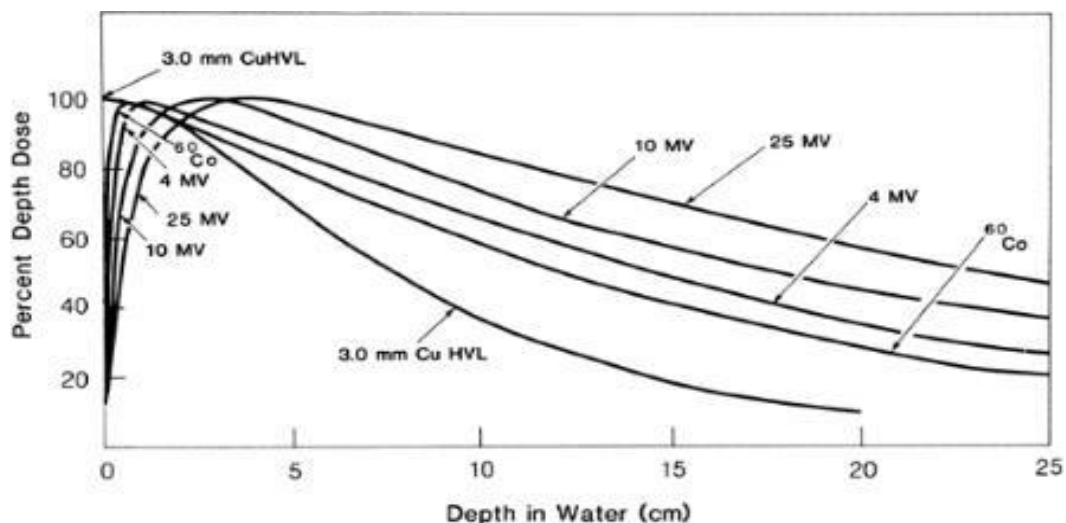


Figure 3: Central axis depth dose distribution for different quality photon beam. (Source: *The Physics of Radiation Therapy* (p. 163), by F. M. Khan, 2003, Philadelphia, PA: Wolters Company. Copyright 2003 by Lippincott Williams and Wilkins.)

## 2.5 Hounsfield Unit

In Computed Tomography (CT), the linear attenuation coefficients ( $\mu$ ) of different anatomical structures are measured and computed to form CT images.<sup>19</sup> Since  $\mu$  is highly energy dependent and the CT x-ray beam is polyenergetic, this makes the direct interpretation of the computed attenuation coefficient values difficult.<sup>19</sup> Therefore, the computed attenuation coefficient is represented as a Hounsfield unit (HU). The HU is a measure of the attenuating properties relative to water. HU is defined for different tissues:

$$HU = \left( \frac{\mu_{\text{tissue}} - \mu_{\text{water}}}{\mu_{\text{water}}} \right) \cdot 1000 ,$$

where  $\mu_{\text{tissue}}$  is the attenuation coefficient of tissues and  $\mu_{\text{water}}$  is the attenuation coefficient of water. The HU for water is 0 HU. The HU value for air can be approximated as having no attenuation, resulting in a value of -1000 HU.<sup>19</sup> Although the HU still retains some dependence on photon energy, since  $\mu_{\text{water}}$  and  $\mu_{\text{tissue}}$  don't necessarily change with photon energy in the same proportion, the primary advantage of HU is that it is much less sensitive to photon energy due to being scaled to water.

## 2.6 Target Volumes

The International Commission on Radiation Units and Measurements (ICRU) in Reports no. 50 and 62 recommended that three target volumes be identified in a treatment plan. Those three target volumes are: Gross Tumor Volume (GTV), Clinical Target Volume (CTV), and Planning Target Volume (PTV).<sup>20</sup>

GTV represents the palpable tumor which is visible in the medical images. CTV surrounds the GTV and includes affected tissue adjacent to the main tumor mass. Lastly, PTV includes both GTV and CTV with additional internal margin that account for the variation of tumor size during therapy, and the movement of the patient.<sup>20</sup>

## 2.7 Current Treatment Modalities

In the past, external beam radiation from a Linac involved a fixed shape aperture where the radiation exited. Advances in technology then lead to the ability to further shape the aperture based on the shape of target at depth. One development was to insert a block. The block is a composite metal made of a Lipowitz's alloy substance containing Bismuth, Lead, Tin, and Cadmium. It melts at around 160° F, permitting its solid form to take shape when it cools. The physical demands of interchanging these blocks lead to the innovation of a multi-leaf collimator (MLC). The MLC is a set of retractable leafs, each made of Tungsten, and 7 cm thick. With an electronic motor, the leafs can individually be driven to shape the aperture as needed. Current technology involves the active motion of these leaves during treatment for static beams at a fixed angle, such as for Intensity Modulated Radiation Therapy (IMRT). However, they can also be used with treatments involving beams that rotate around the patient, such as with Volumetric Modulated Arc Therapy (VMAT). Both of these treatment modalities use modern computer-controlled intensity modulated systems that make use of the multileaf collimator Figure 4.



Figure 4: Dynamic multileaf collimators

In IMRT treatments multiple fields can be applied through a step and shoot method. The entire plan is divided into different beams, each with a set of shapes that the MLC must form during treatment. As the machine transitions from one gantry angle to another, the radiation beam is turned off.<sup>14</sup> The VMAT treatment method is similar to IMRT in that each beam has a set of shapes that the MLC must form during treatment. However, there is no lag in transition as there is no defined angle that the beam must stop. The machine is constantly rotating around the patient. The only caveat is that the shape formed by the MLC must be precise at the desired angle during rotation. The machine is constantly moving and so is the MLC.<sup>14</sup> Like IMRT, VMAT can reduce the treatment time, yet VMAT is more efficient. One VMAT beam can do the same thing that 179 IMRT beams can do, or comparatively with 179 conformal beams that use metal alloy blocks that need interchanged.

### **3.0. METHODS AND MATERIALS**

#### **3.1 Planning**

The treatment delivery considered in this research was given using a Varian<sup>®</sup> Model TrueBeam<sup>®</sup> linear accelerator (LINAC) operating at 6 MV. It possessed a Varian<sup>®</sup> Model NDS120<sup>®</sup> 120 multi-leaf collimator. This research addresses the modern delivery technique of Volumetric Modality Arc Therapy (VMAT). More specifically, this method of delivery is known as Varian<sup>®</sup> RapidArc<sup>®</sup>, as it is intended for use with a Varian LINAC.

The goal of this study was to evaluate the impact of the treatment couch on the dose distribution. Therefore, it is important to identify the dosimetric consequences of modeling the couch in the planning process, since treatment of the patient involves some of the beam potentially passing through the plastic couch that they lay on. To achieve this goal, four treatment plans were selected that each ignored the treatment couch during the planning process. For simplicity in labeling here, I have chosen to refer to these plans as “Excluded couch plans”. The Varian<sup>®</sup> Model Eclipse<sup>®</sup> treatment planning system was used for the calculation of absorbed dose distributions in those plans without including attenuation from the treatment couch. In this study, those plans were copied to insure identical geometry and then the treatment couch was inserted. After the couch was inserted, the Eclipse<sup>®</sup> treatment planning system was made to re-optimize gantry and leaf motion files and then re-calculate the dose distribution again. I refer to those new plans



as” Couch included plans”. Therefore, each patient had two plans; a Couch excluded plan and a Couch included plan. The only difference between these two plans are the absence or the presence of the couch. Differences in the dose distribution and or statistics referenced from dose-volume histogram (DVH) analysis are investigated to determine the consequences of couch incorporation.

### **3.2 Procedure**

#### **3.2.1 Patient selection and the cases descriptions**

Four head and neck cancer patients were randomly selected. Two patients had squamous cell carcinoma at the base of the tongue, with a disease classification Stage II (T2, N0, M0) for both cases. The third patient has the squamous cell carcinoma of the lower neck, with disease classification Stage III (T3, N0, M0). The last patient has the squamous cell carcinoma of the left tonsil with disease classification IV (T3, N2, M0). Therefore, all of the patients have a bit different disease progression. Still, there is something that can be said about the general consequences of target and normal organ coverage when planned nearly identically.

#### **3.2.2 Treatment Plan Set up**

Patient’s CT images are imported to the eclipse treatment planning system. Then, both target structures and organs at risk (OARs) around the tumor were identified on the CT images. After that, the dose constraints are input on the TPS. In the case of the couch included plan, the IGRT is inserted. The final step is the optimization process where the TPS works out the gantry angles, rotation rates and MLC settings to achieve the dose constraints or in other word the TPS objectives.

### **3.2.2.1 Contouring both Target Structures and OARs**

Using a computerized treatment planning system, and making use of the patient's CT scan data, the board certified medical physicist or their dosimetrist assistant uses outlining tools to contour all normal structures. Since these structures are at risk for radiation exposure and possibly some toxicity (functional affects), each are referred to as an organ at risk (OAR). The radiation oncologist is responsible for contouring of tumor volumes or other principal target structures, such as a nerve. For all patients, the clinical target volume (CTV 70) with 5-mm margin was created around the gross tumor volume (GTV). The planning target volume (PTV 70) for CTV 70 was created with 3-mm margin from the CTV 70 to account for the set-up uncertainties and daily repositioning errors. Margins were chosen by the radiation oncologist to account for physiological factors such as patient breathing. The secondary target was the CTV of lymph node chain with high risk, named as CTV 63. PTV 63 with 3-mm margin was created from the CTV 63. The third target was CTV 56, accounting for the lymph node with lower risk. The 3-mm margin that was given to CTV 56 to create PTV 56. The critical structures included the spinal cord, and parotid glands, and other adjacent organs local to the target PTV structures (Figures 5 and 6).

All plans were generated for a treatment in 35 fractions, to deliver total dose of 70 Gy, 63 Gy, and 56 Gy to PTV 70, PTV 63, and PTV 56 respectively. These plans did not include the couch top when the Eclipse® treatment planning system calculated the dose distribution.

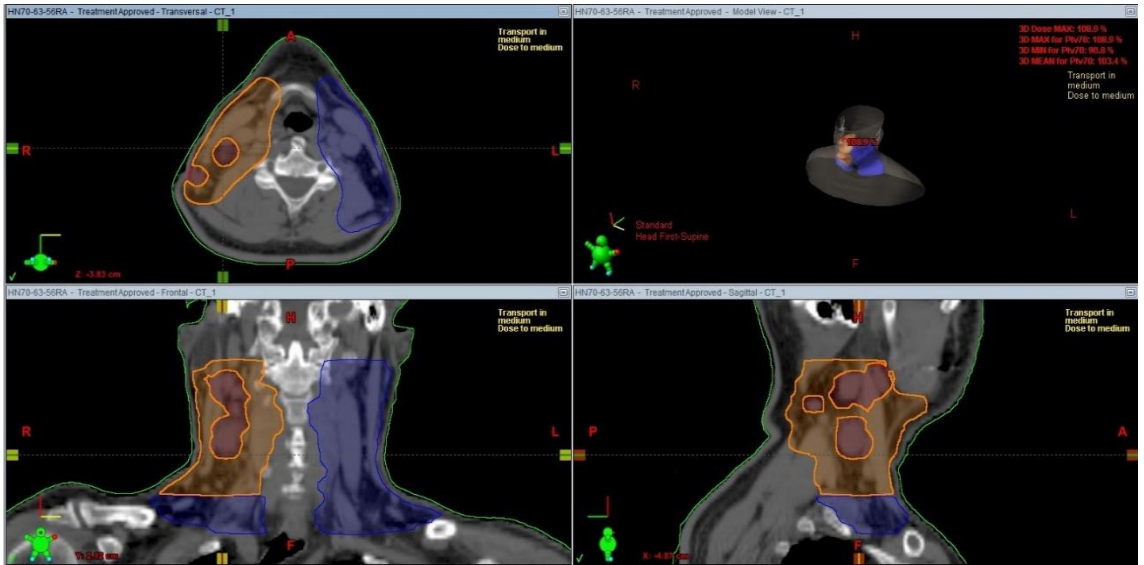


Figure 5: CT image of the tongue base with target structures (red area is PTV 70, orange area is PTV 63, and blue area is PTV 56)

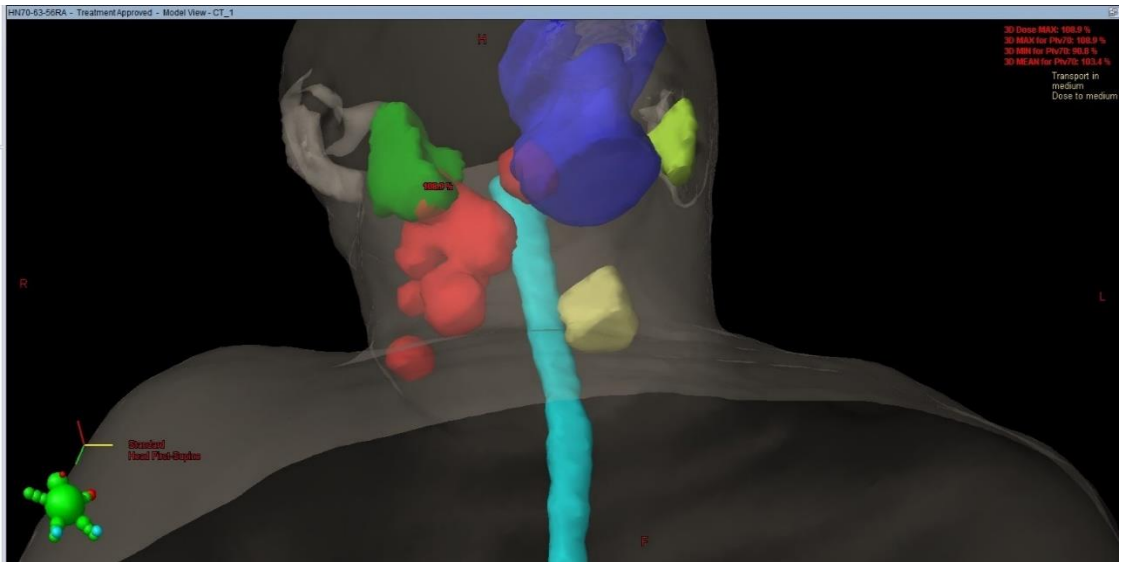


Figure 6: CT image of the tongue base case with normal organs (green area is R. Parotid, blue area is oral cavity, sky blue area is spinal cord, and yellow area is larynx, and light green area is L. Parotid)

### 3.2.2.2 Dose Constraints for Target Structures and OARs

The dose constraints for the target structures and organs at risk are summarized in table 1, and 2.

<b>Target structures</b>	<b>Parameter</b>	<b>Dose % limit [% of 70 Gy]</b>
<b>PTV 70</b>	D <sub>99</sub>	97
	D <sub>95</sub>	99
<b>PTV 63</b>	D <sub>99</sub>	87
	D <sub>95</sub>	89
<b>PTV 56</b>	D <sub>99</sub>	77
	D <sub>95</sub>	79

Table 1: Target structures dose constraints

<b>Organs at risk</b>	<b>Parameter</b>	<b>Dose % limit [% of 70 Gy]</b>
<b>Spinal cord</b>	Max dose	< 64
<b>Brain stem</b>	Max dose	< 64
<b>Mandible</b>	D <sub>30</sub>	< 93
<b>L. Parotid</b>	Mean	< 35
<b>R. Parotid</b>	Mean	< 35
<b>Larynx</b>	Mean	< 79

Table 2: OARs dose constraints

### 3.2.2.3 Inserting the IGRT Couch on the Couch Excluded Plans

The couch considered in this study is the Varian® IGRT Couch Top®. It is made of a carbon fiber superficial shell and a radio-transparent foam filling the internal cavity. This couch is manufactured with three thicknesses (thin, middle, thick) increasing from the section of the couch used for head treatments (right side as illustrated in Figure 7) towards the section used for abdomen treatments. Even though the lower portion of the couch resembles that of an inclined plane with a shallow angle, the couch is uniquely designed with a six-degrees-of-freedom (6DOF) stepper system, enabling a flat upper surface for patient positioning, no matter what weight distribution the patient has. The couch can maneuver laterally, longitudinally, vertically, as well as with rotation, pitch and roll. The black board on the figure below is the couch top. For most treatments, it is through this board that some radiation is required to pass.



Figure 7: The Varian® IGRT Couch Top®

The Eclipse<sup>®</sup> treatment planning system allows the board certified medical physicist to incorporate the IGRT Couch Top<sup>®</sup> in treatment plans if desired. The CT images for the four patients did not include the couch when they were treated in the past. In order to apply the couch into the planning process, plans were first copied, where the couch structure could be inserted. The only way to represent the Varian<sup>®</sup> IGRT Couch Top<sup>®</sup> on CT images is to assign appropriate values of Hounsfield units to the couch structure, on every slice, at precisely the location of the structure. In this manner, the planning system would be able to recognize the couch possesses a density, from which to estimate attenuation. Since the Varian<sup>®</sup> IGRT Couch Top<sup>®</sup> has two parts, the external carbon fiber shell and the internal foam filler material, the outer surface was given 700 HU and for the internal foam -960 HU. These values were verified by the board certified medical physicist during the machine and planning system commissioning process, prior to this research. Implementation of the couch in the planning system is shown in figure below.

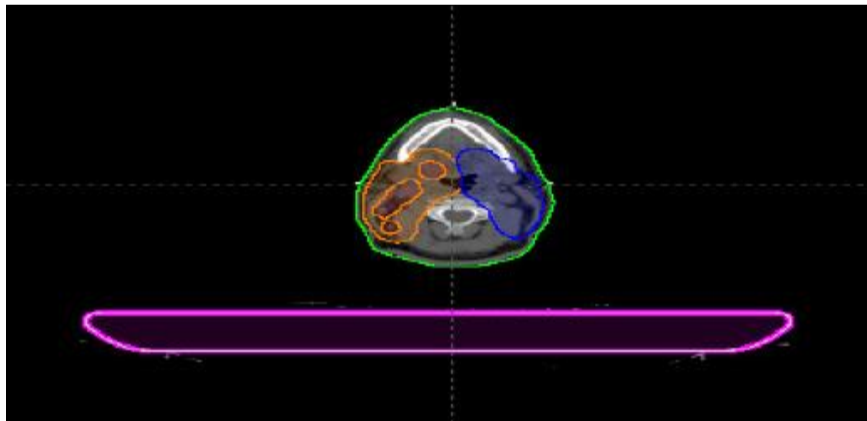


Figure 8: The IGRT couch model in Eclipse (the couch in pink color after being inserted in the patient CT image)

Once the IGRT couch inserted in the CT images of couch excluded plans, the dose distributions were then recalculated. Dose statistics were then reviewed along with the distribution of dose in all planes for analysis.

### **3.3 Dose Distribution Analysis**

Quantitative evaluation of the DVH for each patient was performed. The DVH provides numerical information of how much dose is absorbed by each percentage of volume for all anatomical structures and targets.<sup>14</sup> On the DVH curve, the vertical axis represents the volume percentage and the horizontal axis is the relative percentage dose (Figure 9). Here, 100% on the x-axis of Figure 9 corresponds to 70 Gy, which is the dose prescribed for PTV 70. For example, a percentage volume of 50% on the y-axis represents half of the structural volume of the organ or target, and the x-axis value for a particular organ receives the stated dose in the plot.

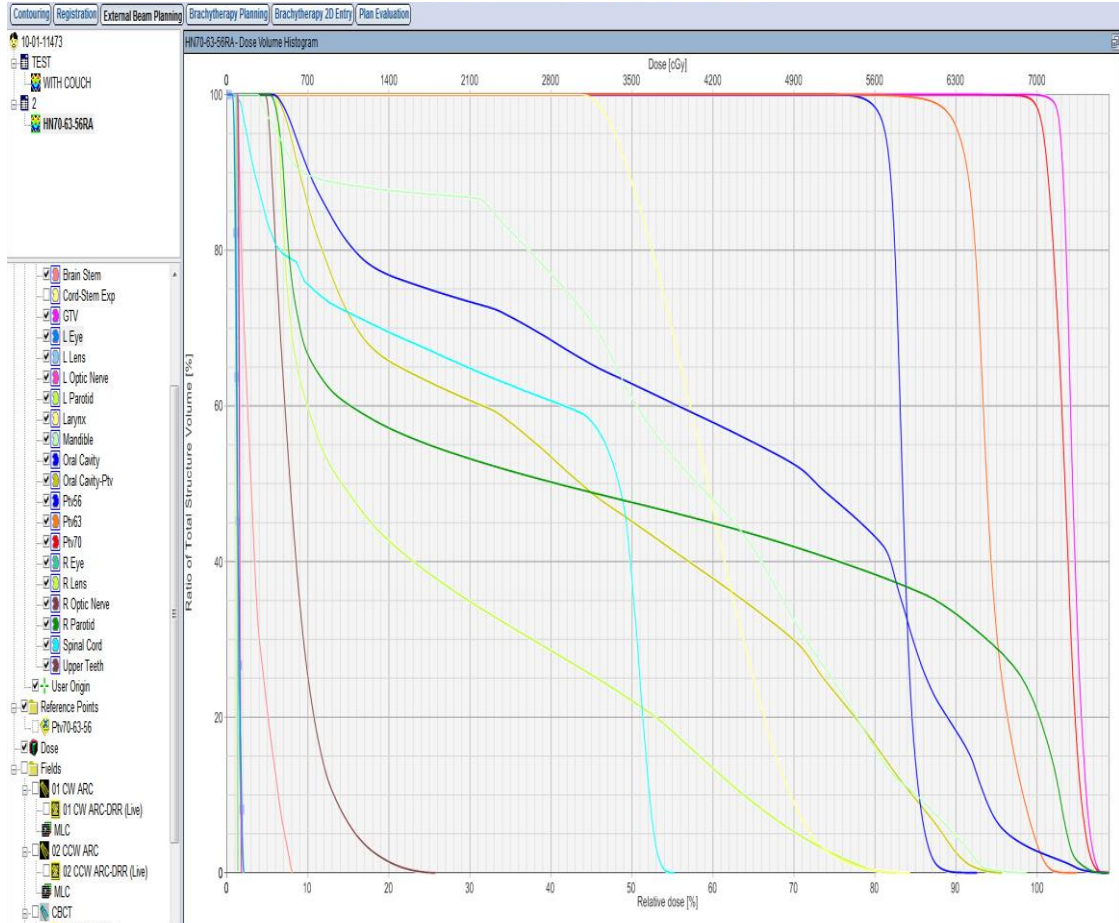


Figure 9: Dose Volume Histogram (DVH) (each color represents an anatomical structure)

For the target structures, the mean dose value was evaluated to assess absorbed dose estimate shifts induced by the couch. The dose covering 95% of the volume of the target structure ( $D_{95\%}$ ) is evaluated to ensure if the Couch included plan still meets treatment planning criteria known as dose-volume constraints (Table 2). Those partial volume dose constraints are decided upon by the radiation oncologist. Values for  $D_{98\%}$ ,  $D_{50\%}$ , and  $D_{2\%}$  are reported to calculate the Homogeneity index (HI). The HI is a ratio used to evaluate the dose homogeneity in a target structure, such as PTV 70. As an example, we consider the homogeneity index for PTV 70 to be calculated from DVH data using the following



calculation:  $HI = (D_{2\%} - D_{98\%}) / D_{50\%}$ . In this format,  $D_{98\%}$ ,  $D_{50\%}$ , and  $D_{2\%}$  represent the dose delivered to 98%, 50%, and 2% of the volume of the PTV 70, respectively.<sup>21</sup> The ideal value of HI is zero, revealing a uniform distribution of dose throughout the entire target. The HI is used as an indicator, hinting that when values stray far from the intended 0 heterogeneity mark, that one should closely observe the actual distribution of dose in each of the CT views.

### **3.4 Beam Attenuation Measurement**

The aim of this experiment was to identify beam attenuation affects when the couch is inserted into patients' treatment plans. First, in order to verify prior research measurements, the impact of gantry angle on beam attenuation was studied with a field size of 10x10cm<sup>2</sup>. The measurement was performed with a Capintec, Inc.® (Florham Park, NJ) Model PR-06C Farmer-type ionization chamber, placed at a depth of 6 cm in a CIRS (Norfolk, VA) Plastic Water® phantom. The measurement setup is illustrated in Figure 10. A Capintec, Inc.® Model 192 electrometer was used to measure the accumulated charge produced in the ion chamber when irradiated. The phantom was aligned longitudinally on the thinner part of the couch. Following that, the couch was raised so as to center of the chamber at the isocenter of the Linac. Attenuation was measured at various angles. One measurement was obtained with the beam set at an angle projecting downward, thus irradiating the ion chamber without first passing through the couch. At the angle opposite the first measurement, another measurement was obtained with the beam set an angle projecting upward. For an upward beam, the couch would need to be penetrated first before the incident x-rays arrive at the ion chamber. A ratio of charge collected between the downward projected beam and the upward projected beam

give rise to the attenuation exhibited at that angle (i.e. 15° versus 165°). The Beam-on time was fixed for all measurements, roughly corresponding to the time to delivery 100 cGy at  $d_{\max}$ .

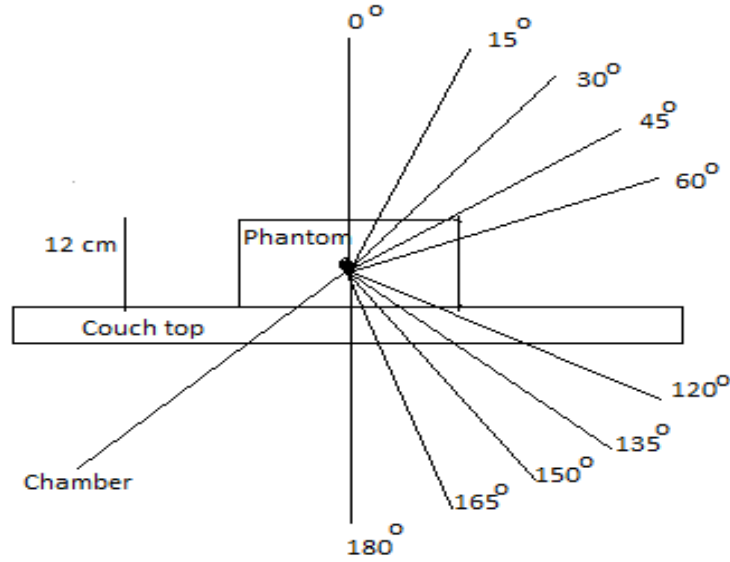


Figure 10: Measurement setup for couchtop beam attenuation

The equation used to calculate the beam attenuation is

$$\frac{\text{Ion chamber reading without couch for an angle} - \text{Ion chamber reading with couch for the opposite angle}}{\text{Ion chamber reading without couch for the angle}}$$

### 3.5 Theoretical Calculations of Couch Attenuation and HU

At 6 Mev, the mass attenuation coefficients are  $0.02469 \text{ cm}^2/\text{g}$  and  $0.0277 \text{ cm}^2/\text{g}$  for carbon and water respectively.<sup>22</sup> The density of carbon fiber is  $1.9 \text{ g/cm}^3$  and the water density is  $1 \text{ g/cm}^3$ .<sup>23</sup> Therefore, the linear attenuation coefficients are  $0.0469 \text{ cm}^{-1}$  and  $0.0277 \text{ cm}^{-1}$  for carbon and water respectively. The thickness of carbon fiber is 0.6 cm for both layers. The following equation was used to calculate the beam attenuation at normal incidence and 120°,

$$I = I_0 e^{-\mu x}$$

the beam attenuation (%) =  $1 - (I / I_0) \times 100$ .

At normal incidence  $x=0.6$  cm and at an angle of incidence of  $120^\circ$ , the effective thickness of the couch is 1.2 cm. In addition, an estimate of HU for the carbon shell was made by using the above linear attenuation coefficients in the equation which defines HU:

$$HU = \left( \frac{\mu_{\text{tissue}} - \mu_{\text{water}}}{\mu_{\text{water}}} \right) \cdot 1000.$$

This calculated value is compared with the value used experimentally.

## 4.0. RESULTS

### 4.1 Results of Beam Attenuation Measurement

The beam attenuation of the IGRT Couch Top® as function of gantry angle is presented in table 3. The highest beam attenuation is 4.24% with a gantry angle of 120°, and the minimum beam attenuation is 2.25% with the gantry angle 180°. These results are close to Vanetti *et al* measurements with attenuation of 2.3% and 3.1% with gantry angles of 180° and 135°, respectively.<sup>13</sup>

Gantry Angle	Measurement (NO Couch) (Coulomb)	Measurement (IGRT Couch) (Coulomb)	Beam Attenuation (%)
0° - 180°	89.0	87.0	2.25
15° - 165°	88.4	86.3	2.38
30° - 150°	86.1	83.8	2.67
45° - 135°	83.2	80.0	3.85
60° - 120°	70.8	67.8	4.24

Table 3: Beam attenuation of IGRT Couch Top® at different angle

### 4.2 Result of Theoretical Calculations of Couch Attenuation and HU

The beam attenuations at 0° - 180° and 60° - 120° are 2.8% and 5.0% which are very close to values found by measurement of corresponding angles in Table 3. The HU of the external shell carbon fiber is 693.5 and this value is similar to the value used in this study of 700.

### 4.3 Patient Results

#### 4.3.1 First patient

The DVH analysis of target structures for the first patient are shown in Table 4. On average, 0.5% (0.35 Gy) of the dose to the PTV 70, and 0.4% of the dose to both PTV 63 and PTV 56 (0.28 Gy) (not shown) were lost.

<b>Organ</b>	<b>PTV 70</b>			<b>PTV 63</b>		
<b>Parameter</b>	<b>Couch Included</b>	<b>Couch Excluded</b>	<b>Diff.</b>	<b>Couch Included</b>	<b>Couch Excluded</b>	<b>Diff.</b>
<b>Max dose [% of 70 Gy]</b>	108.4	108.9	-0.5	106.0	104.9	1.1
<b>Mean dose [% of 70 Gy]</b>	102.9	103.4	-0.5	93.8	94.2	-0.4
<b>D<sub>99%</sub> [% of 70 Gy]</b>	98.0	99.0	-1.0	87.0	89.0	-2.0
<b>D<sub>95%</sub> [% of 70 Gy]</b>	99.5	101.0	-1.5	88.5	90.5	-2.0

Table 4: First patient DVH analysis for the targets structures

The Homogeneity Index (HI) of PTV 70 for the two plans are shown in Table 5.

<b>Plan type</b>	<b>D<sub>2%</sub></b>	<b>D<sub>50%</sub></b>	<b>D<sub>98%</sub></b>	<b>HI</b>
<b>Couch Included</b>	74.55	72.1	69.3	0.0728
<b>Couch Excluded</b>	74.62	72.45	70	0.0638

Table 5: Homogeneity Index (HI) of PTV 70 for the first patient

The results of the DVH analysis for some organs at risk for the first patient are summarized in Table 6.

<b>Organ</b>	<b>Parameter</b>	<b>Couch Included</b>	<b>Couch Excluded</b>	<b>Difference</b>
<b>Mandible</b>	<b>Max dose [%]</b>	100.0	98.7	1.3
	<b>Mean dose [%]</b>	55.2	55.5	-0.3
	<b>D<sub>80</sub> [%]</b>	39.5	37.0	2.5
	<b>D<sub>30</sub> [%]</b>	71.5	71.5	0.0
<b>Oral cavity</b>	<b>Max dose [%]</b>	107.0	108.5	-1.5
	<b>Mean dose [%]</b>	60.0	59.5	0.5
	<b>D<sub>65</sub> [%]</b>	47.5	45.0	2.5
	<b>D<sub>45</sub> [%]</b>	80.5	78.0	2.5
<b>Spinal cord</b>	<b>Max dose [%]</b>	56.3	55.3	1.0
	<b>Mean dose [%]</b>	34.4	35.0	-0.6
	<b>D<sub>65</sub> [%]</b>	32.5	30.0	2.5
	<b>D<sub>45</sub> [%]</b>	47.0	49.5	-2.5
<b>Larynx</b>	<b>Max dose [%]</b>	86.5	84.3	2.2
	<b>Mean dose [%]</b>	63.5	59.6	3.9
	<b>D 90 [%]</b>	56.0	49.5	6.5
	<b>D 40 [%]</b>	64.5	61.5	3.0
<b>L Parotid</b>	<b>Max dose [%]</b>	80.3	82.6	-2.3
	<b>Mean dose [%]</b>	25.4	26.4	-1.0

Table 6: First patient DVH analysis for some organs at risk

For the mandible, the maximum dose which covered less than 1% of the whole organ's volume increased by 1.3% (0.9 Gy).  $D_{80}$  is the dose covered 80% of the mandible's volume and it increased by 2.5% (1.75 Gy). The dose distribution difference for the mandible is shown on Figure 11 below.

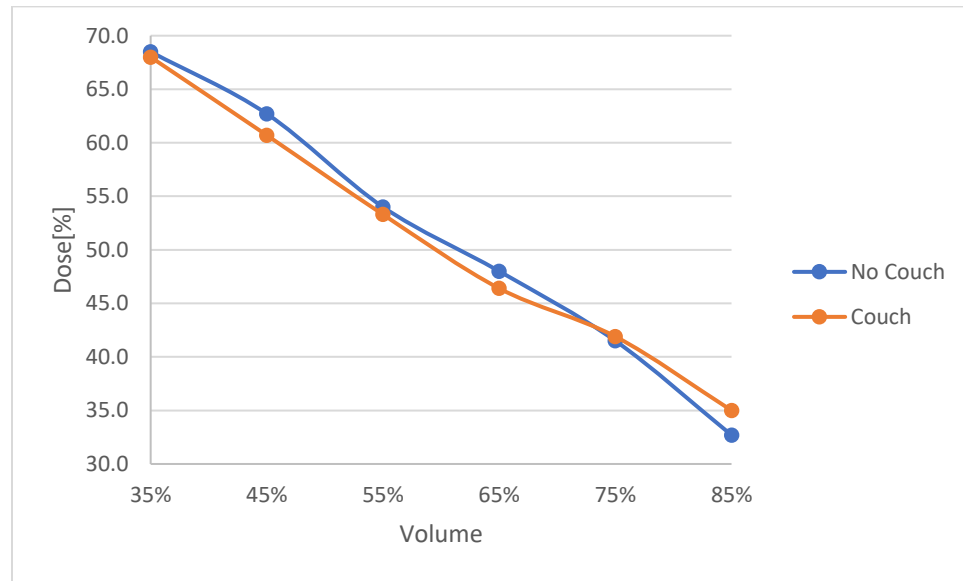


Figure 11: Does percentage distribution for mandible between 85% and 35% of the volume

The dose which is covered the oral cavity when couch being inserted slightly increased in two areas from 71% to 62% and 50% to 10% otherwise both scenarios are almost identical.

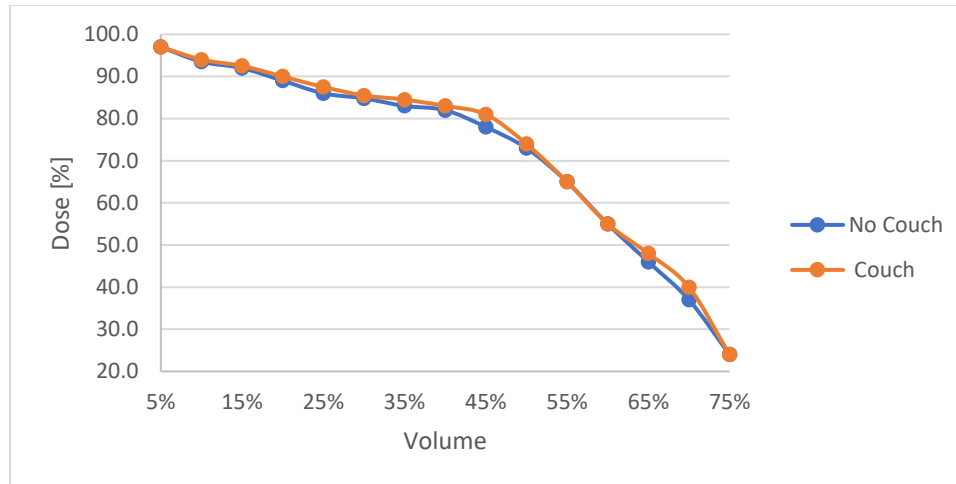


Figure 12: Does percentage distribution for oral cavity between 75% and 5% of the volume

The volume of spinal cord which is covered by 50% of the prescribed dose (35 Gy) dropped from 37% to 25% for the couch excluded plan as shown in the figure below.

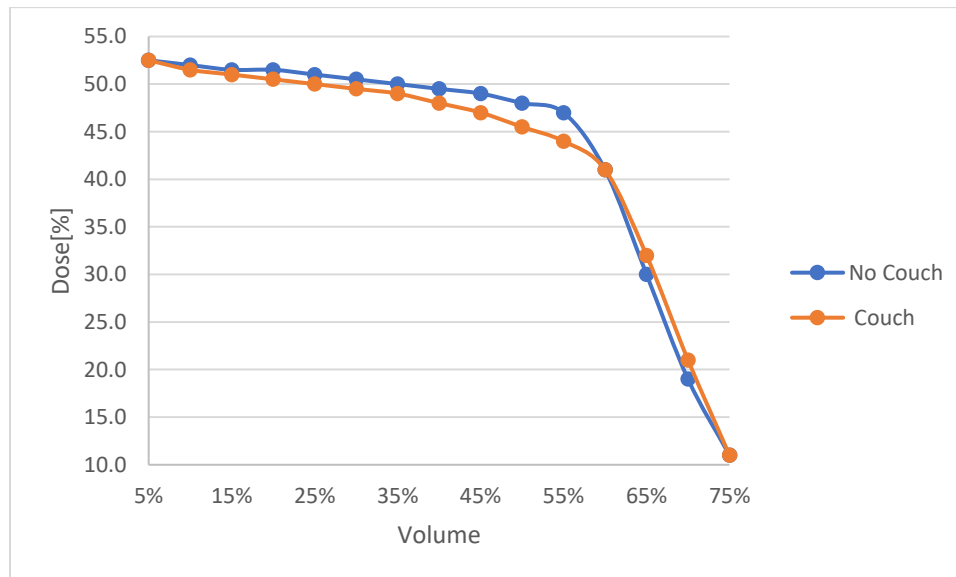


Figure 13: Does percentage distribution for spinal cord between 75% and 5% of the volume

For the larynx, the dose discrepancy is more relevant and reach as high as 4.5 Gy. However, the mean dose with 63.5% is still less than the constraint which is less than 79% of the prescribed dose.



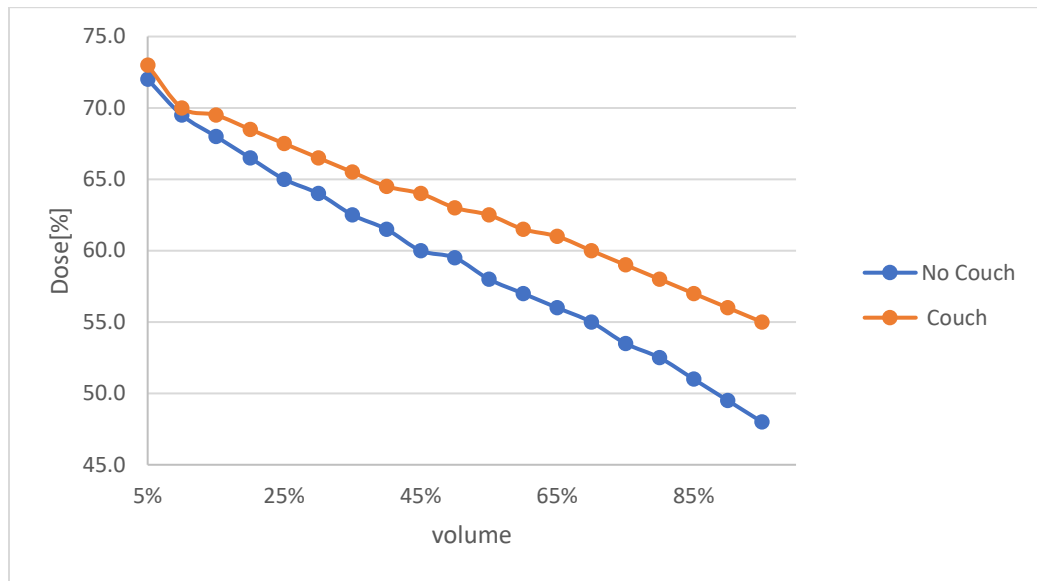


Figure 14: Does percentage distribution for larynx between 95% and 5% of the volume

#### 4.3.2 Second Patient

The DVH of target structures for the third patient are shown in Table 7. The average dose losses by target structures are 0.8% (0.56 Gy), 0.9% (0.63 Gy), and 1.2% (0.84 Gy) for PTV 70, PTV 63 and PTV 56 (not shown) respectively.

<b>Organ</b>	<b>PTV 70</b>			<b>PTV 63</b>		
<b>Parameter</b>	<b>Couch Included</b>	<b>Couch Excluded</b>	<b>Diff.</b>	<b>Couch Included</b>	<b>Couch Excluded</b>	<b>Diff.</b>
<b>Max dose [%]</b>	108.9	112.4	-3.5	104.6	104.2	0.4
<b>Mean dose [%]</b>	102.9	103.7	-0.8	93.2	94.1	-0.9
<b>D<sub>99%</sub> [%]</b>	98.0	99.0	-1.0	87.0	88.0	-1.0
<b>D<sub>95</sub> [%]</b>	99.5	101.0	-1.5	89.0	90.5	-1.5

Table 7: Second patient DVH analysis for the targets structures

The Homogeneity Index (HI) of PTV 70 for the two plans are shown in Table 8.

<b>Plan type</b>	<b>D<sub>2%</sub></b>	<b>D<sub>50%</sub></b>	<b>D<sub>98%</sub></b>	<b>HI</b>
<b>Couch Included</b>	74.2	72.24	67.2	0.0969
<b>Couch Excluded</b>	74.97	72.73	69.3	0.0779

Table 8: Homogeneity Index (HI) of PTV 70 for the second patient

The results of the DVH analysis for some organs at risk which the effects are statistically significant and more visible for the third patient are summarized in Table 9.

Organ	Parameter	Couch Included	Couch Excluded	Difference
Mandible	Max dose [%]	96.8	96.5	0.3
	Mean dose [%]	19.1	19.6	-0.5
	D <sub>30</sub> [%]	31.0	32.0	-1.0
Oral cavity	Max dose [%]	96.7	99.2	-2.5
	Mean dose [%]	28.5	29.0	-0.5
	D <sub>35</sub> [%]	39.0	41.5	-2.5
Spinal cord	Max dose [%]	56.5	57.6	-1.1
	Mean dose [%]	22.5	22.2	0.3
	D <sub>30</sub> [%]	44.0	42.0	2.0

Table 9: Second patient DVH analysis for some organs at risk

For the mandible and the oral cavity, the mean doses of the couch excluded plans are 0.35Gy lower than the mean dose of the Couch included plans.

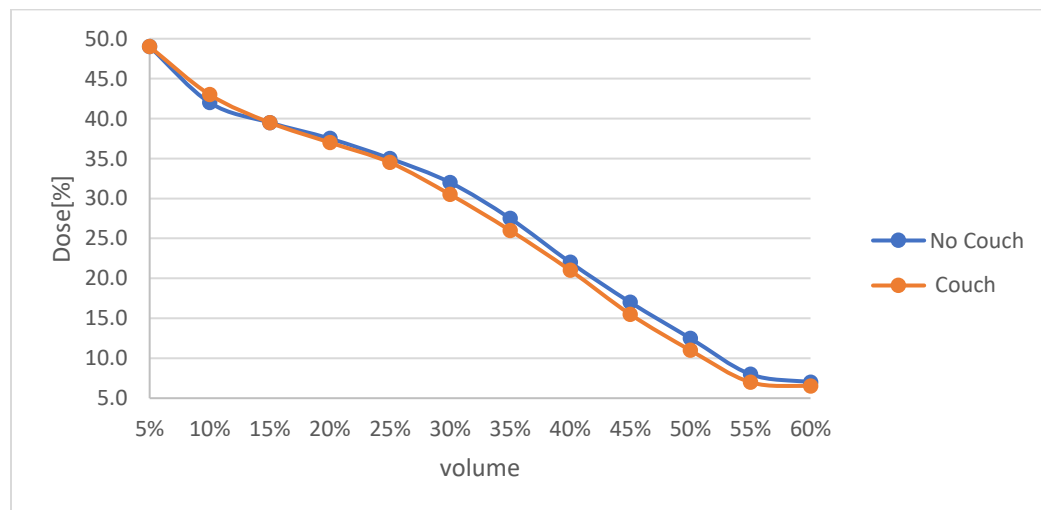


Figure 15: Does percentage distribution for mandible between 60% and 5% of the volume

The dose which is covered from 40% to 20% of spinal cord volume increased as couch included and reach its maximum with 1.4 Gy higher than the couch excluded plan.

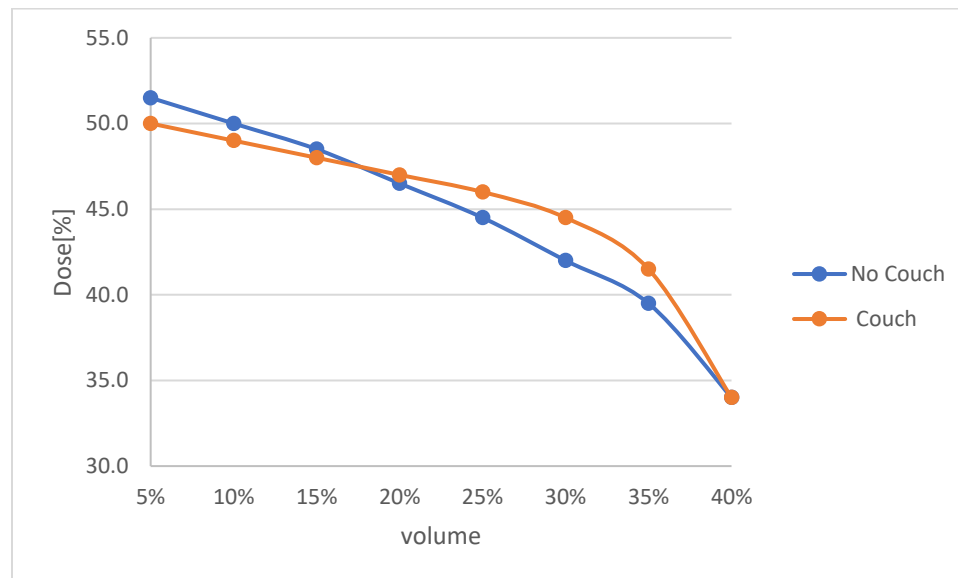


Figure 16: Does percentage distribution for spinal cord between 40% and 5% of the volume

### 4.3.3 Third Patient

The dose statistics of target structures for the third patient are shown in Table 10.

On average, 0.9% of the dose to the PTV 70, 1.3% of the dose to PTV 63 and 0.7% of the dose to PTV 56 (not shown) were lost.

<b>Organ</b>	<b>PTV 70</b>			<b>PTV 63</b>		
<b>Parameter</b>	<b>Couch Included</b>	<b>Couch Excluded</b>	<b>Diff.</b>	<b>Couch Included</b>	<b>Couch Excluded</b>	<b>Diff.</b>
<b>Max dose [%]</b>	111.9	113.6	-1.7	107.4	111.4	-4.0
<b>Mean dose [%]</b>	105.6	106.5	-0.9	95.3	96.6	-1.3
<b>D<sub>99%</sub> [%]</b>	100.0	101.0	-1.0	87.0	88.0	-1.0
<b>D<sub>95</sub> [%]</b>	102.0	103.0	-1.0	90.0	91.0	-1.0

Table 10: Third patient DVH analysis for the targets structures

The Homogeneity Index (HI) of PTV 70 for the two plans are shown in Table 11.

<b>Plan type</b>	<b>D<sub>2%</sub></b>	<b>D<sub>50%</sub></b>	<b>D<sub>98%</sub></b>	<b>HI</b>
<b>Couch Included</b>	76.65	74.2	70.7	0.0802
<b>Couch Excluded</b>	77.35	74.69	71.05	0.0843

Table 11: Homogeneity Index (HI) of PTV 70 for the third patient

The results of the DVH analysis for some organs at risk for the third patient are shown in Table 12.

<b>Organ</b>	<b>Parameter</b>	<b>Couch Included</b>	<b>Couch Excluded</b>	<b>Difference</b>
<b>Mandible</b>	<b>Max dose [%]</b>	111.9	109.6	2.3
	<b>Mean dose [%]</b>	55.4	56.1	-0.7
	<b>D<sub>80</sub></b>	38.5	41.5	-3.0
<b>R Parotid</b>	<b>Max dose [%]</b>	83.2	86.5	-3.3
	<b>Mean dose [%]</b>	32.9	37.5	-4.6
	<b>D<sub>60</sub></b>	26.0	31.0	-5.0
	<b>D<sub>30</sub></b>	38.0	45.5	-7.5
<b>Spinal cord</b>	<b>Max dose [%]</b>	60.1	67.1	-7.0
	<b>Mean dose [%]</b>	37.3	40.4	-3.1
	<b>D<sub>75</sub></b>	25.0	28.0	-3.0
	<b>D<sub>20</sub></b>	51.5	57.5	-6.0
<b>Larynx</b>	<b>Max dose [%]</b>	89.3	90.8	-1.5
	<b>Mean dose [%]</b>	62.6	66.9	-4.3
	<b>D<sub>80</sub></b>	55.5	60.5	-5.0
<b>L Parotid</b>	<b>Max dose [%]</b>	98.6	103.8	-5.2
	<b>Mean dose [%]</b>	27.7	30.2	-2.5
	<b>D<sub>20</sub></b>	53.0	59.5	-6.5
<b>R brachial plexus</b>	<b>Max dose [%]</b>	85.1	86.4	-1.3
	<b>Mean dose [%]</b>	56.0	53.5	2.5
	<b>D<sub>70</sub></b>	40.0	33.0	7.0
<b>Oral cavity</b>	<b>Max dose [%]</b>	95.6	99.1	-3.5
	<b>Mean dose [%]</b>	44.3	45.6	-1.3

Table 12: Third patient DVH analysis for some organs at risk

For the mandible, the mean dose is dropped by 0.5 Gy and the main difference is occurred on the dose covered 80% of the mandible volume which is decreased by 2.1 Gy.

The dose difference is more relevant for the right parotid gland and reach as high as 5.25 Gy which is covered 30% of the volume as shown on the figure below. The mean dose dropped by 3.22 Gy.

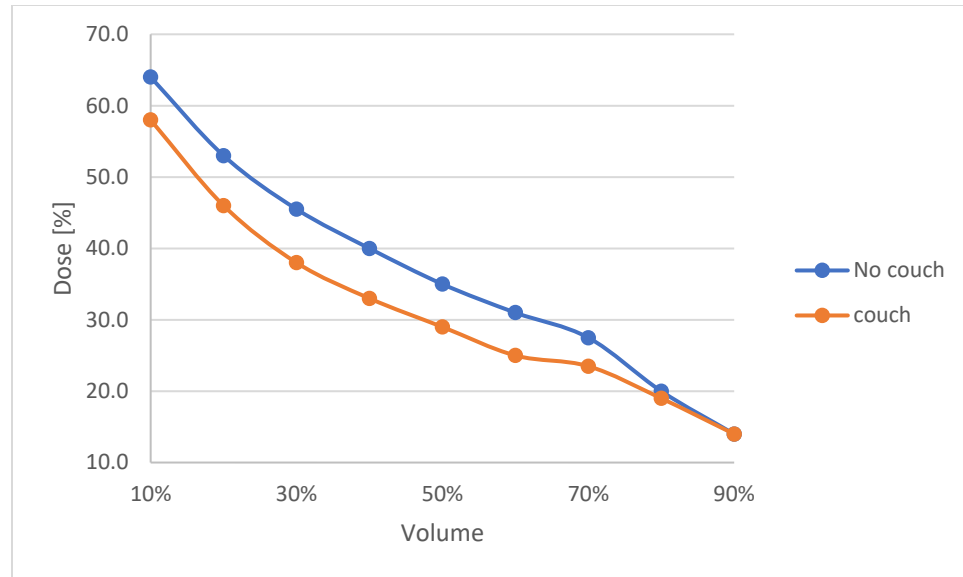


Figure 17: Does percentage distribution for right parotid gland between 90% and 10% of the volume

The mean dose dropped by 2.17 Gy for the spinal cord and 4.2 Gy higher for the dose covered 20% of the volume.

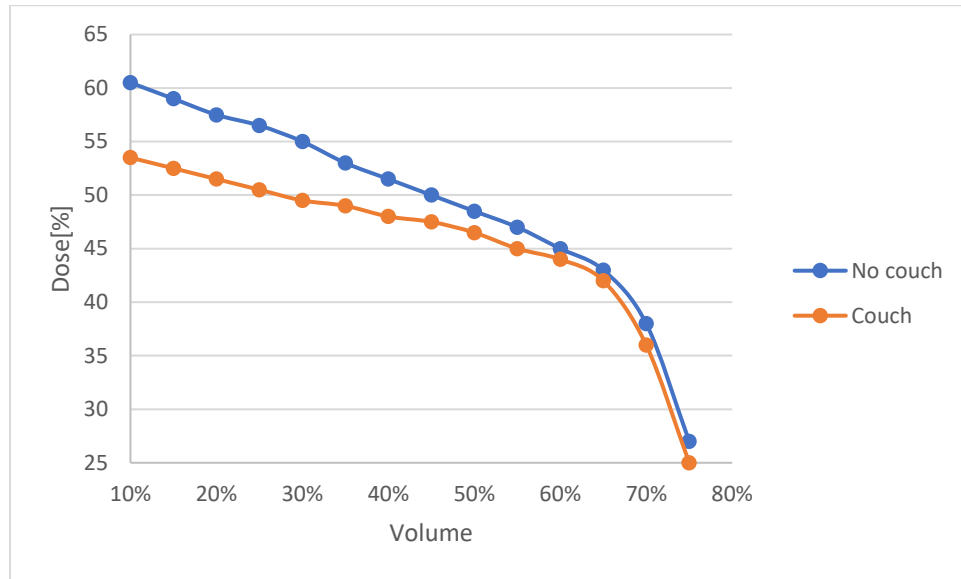


Figure 18: Does percentage distribution for spinal cord between 75% and 10% of the volume

The dose discrepancy for the larynx is more visible and the mean dose decreased by 3.01 Gy. The maximum difference occurred for the dose that covered 70% of the volume and reach 3.85 Gy.

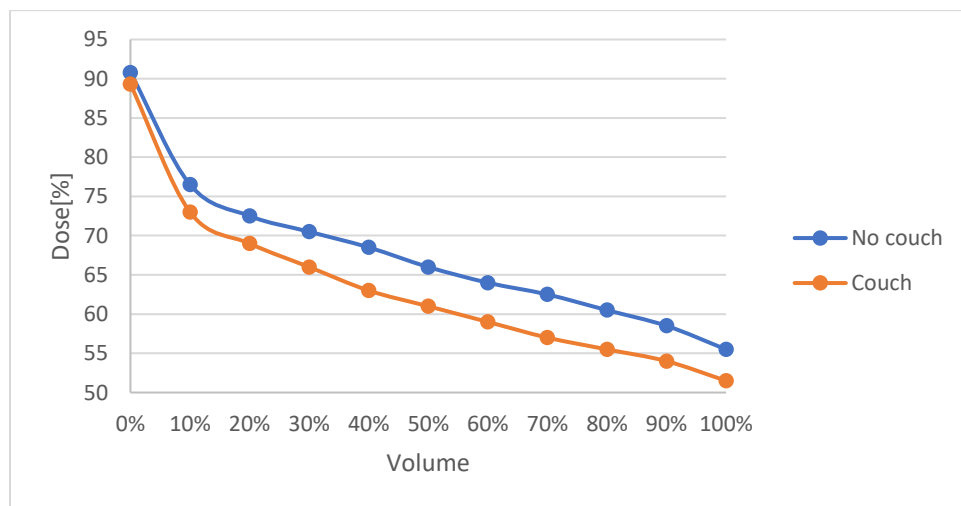


Figure 19: Does percentage distribution for larynx



For the left parotid gland, the mean dose dropped by 1.75 Gy and the significant difference is 4.55 Gy for the dose covered 20% of the volume.

The mean dose increased by 1.75 Gy and the dose difference between the two scenarios are mainly occurred on the dose covered from 40% to 90% of the right brachial plexus.

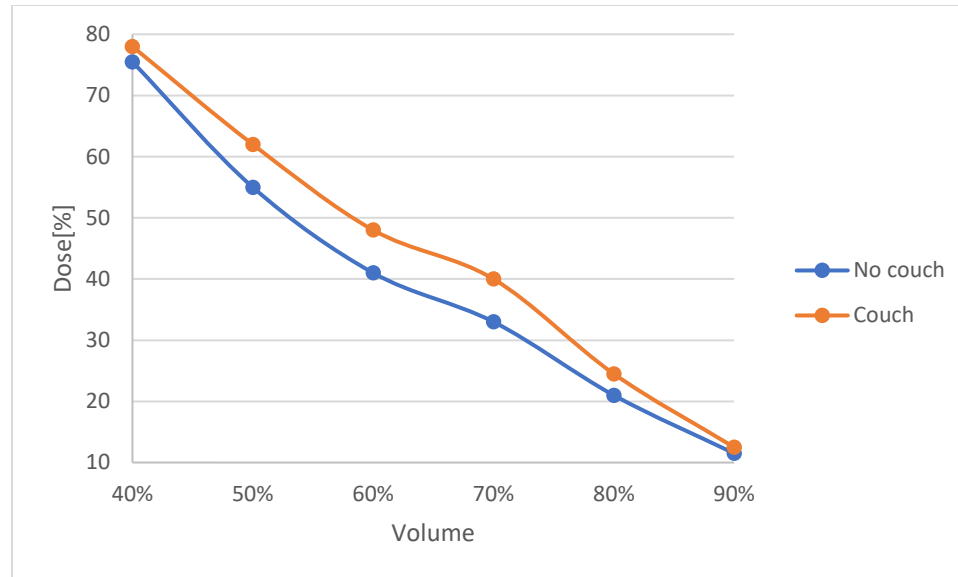


Figure 20: Does percentage distribution for right brachial plexus between 90% and 40% of the volume

#### 4.3.4 Fourth Patient

The DVH of target structures for the fourth patient are shown in Table 13. The average dose losses by target structures are 0.9% (0.63 Gy), 1.1% (0.77 Gy), and 0.6% (0.42 Gy) for PTV 70, PTV 63 and PTV 56 (not shown) respectively.

<b>Organ</b>	<b>PTV 70</b>			<b>PTV 63</b>		
<b>Parameter</b>	<b>Couch Included</b>	<b>Couch Excluded</b>	<b>Diff.</b>	<b>Couch Included</b>	<b>Couch Excluded</b>	<b>Diff.</b>
<b>Max dose [%]</b>	112.2	112.3	-0.1	104.8	107.2	-2.4
<b>Mean dose [%]</b>	104.2	105.1	-0.9	94.3	95.4	-1.1
<b>D<sub>99%</sub> [%]</b>	98.0	99.0	-1.0	87.0	88.0	-1.0
<b>D<sub>95</sub> [%]</b>	100.0	100.5	-0.5	88.5	90.0	-1.5

Table 13: Fourth patient DVH analysis for the targets structures

The Homogeneity Index (HI) of PTV 70 for the two plans are shown in Table 14.

<b>Plan type</b>	<b>D<sub>2%</sub></b>	<b>D<sub>50%</sub></b>	<b>D<sub>98%</sub></b>	<b>HI</b>
<b>Couch Included</b>	76.3	73.15	68.6	0.1053
<b>Couch Excluded</b>	76.65	73.64	68.6	0.1093

Table 14: Homogeneity Index (HI) of PTV 70 for the fourth patient

The results of the DVH analysis for some organs at risk for the fourth patient are shown in Table 15.

<b>Organ</b>	<b>Parameter</b>	<b>Couch Included</b>	<b>Couch Excluded</b>	<b>Difference</b>
<b>R Parotid</b>	<b>Max dose [%]</b>	109.0	109.8	-0.8
	<b>Mean dose [%]</b>	60.9	61.7	-0.8
<b>Spinal cord</b>	<b>Max dose [%]</b>	63.2	68.3	-5.1
	<b>Mean dose [%]</b>	42.6	45.4	-2.8
	<b>D<sub>65</sub></b>	48.0	52.5	-4.5
	<b>D<sub>30</sub></b>	55.0	59.0	-4.0
<b>Larynx</b>	<b>Max dose [%]</b>	90.9	93.3	-2.4
	<b>Mean dose [%]</b>	66.8	69.2	-2.4
	<b>D<sub>90</sub></b>	55.5	59.0	-3.5
<b>L Parotid</b>	<b>Max dose [%]</b>	93.3	91.3	-2.0
	<b>Mean dose [%]</b>	28.9	30.9	-2.0
	<b>D<sub>30</sub></b>	35.5	40.0	-4.5
<b>R brachial plexus</b>	<b>Max dose [%]</b>	82.4	82.7	-0.3
	<b>Mean dose [%]</b>	67.2	67.7	-0.5
<b>L brachial plexus</b>	<b>Max dose [%]</b>	83.0	84.2	-1.2
	<b>Mean dose [%]</b>	55.2	55.4	-0.3
	<b>D<sub>45</sub></b>	75.0	72.0	-3.0

Table 15: Fourth patient DVH analysis for some organs at risk

The dose covered until 70% of the right parotid gland volume is almost identical, however the mean dose dropped by 0.56 Gy.

For the spinal cord, the mean dose decreased by 1.96 Gy and the discrepancies are more visible for the doses covered from 70% to 10% as shown on the figure below.

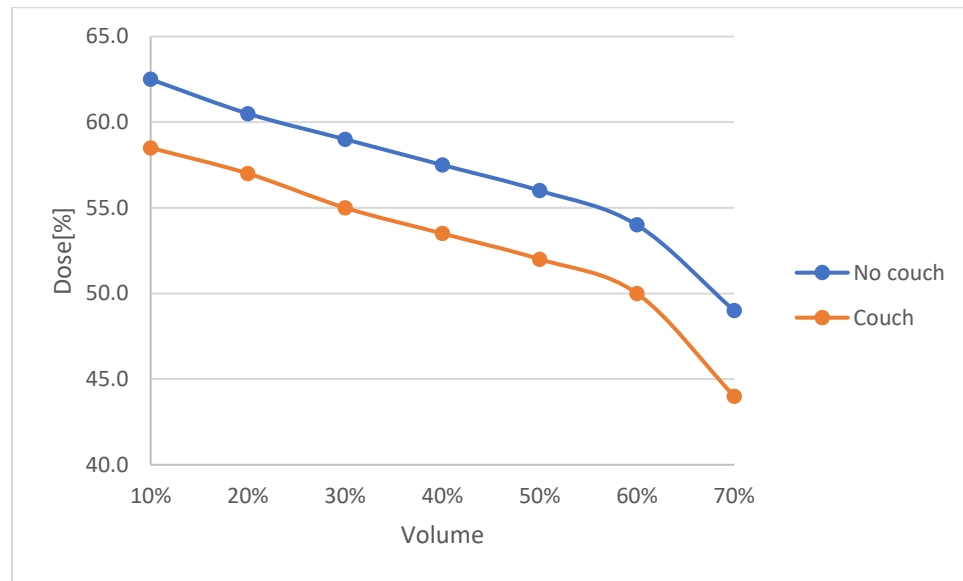


Figure 21: Does percentage distribution for spinal cord between 70% and 10% of the volume

For the larynx, the mean dose dropped by 1.68 Gy and the biggest difference between the two scenarios occurred for the dose covered 90% of the volume.

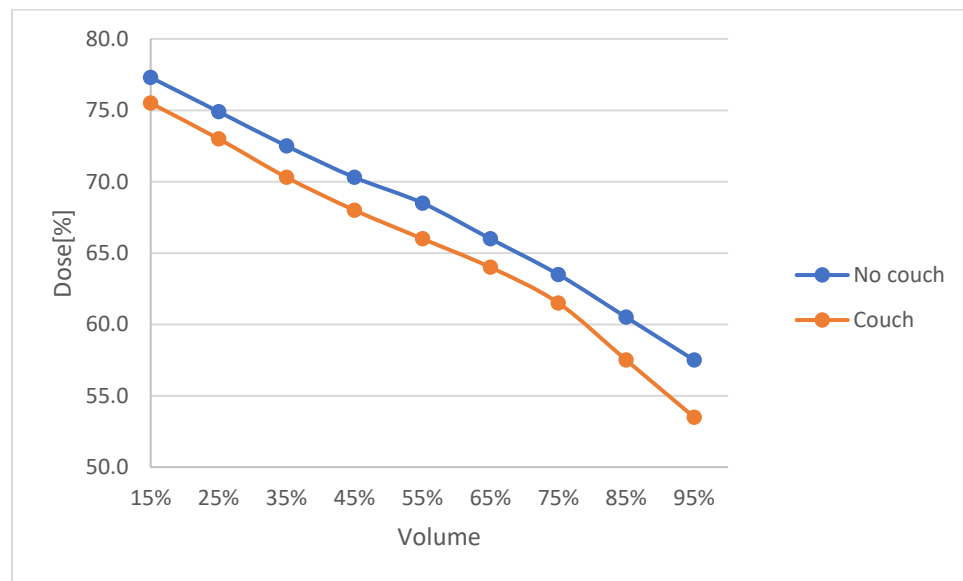


Figure 22: Does percentage distribution for larynx between 95% and 15% of the volume

The dose discrepancy for the left parotid gland between the two planes is visible for the doses covered between 70% and 5% of the volume otherwise both planes are superimposed. The mean dose decreased by 1.4 Gy.

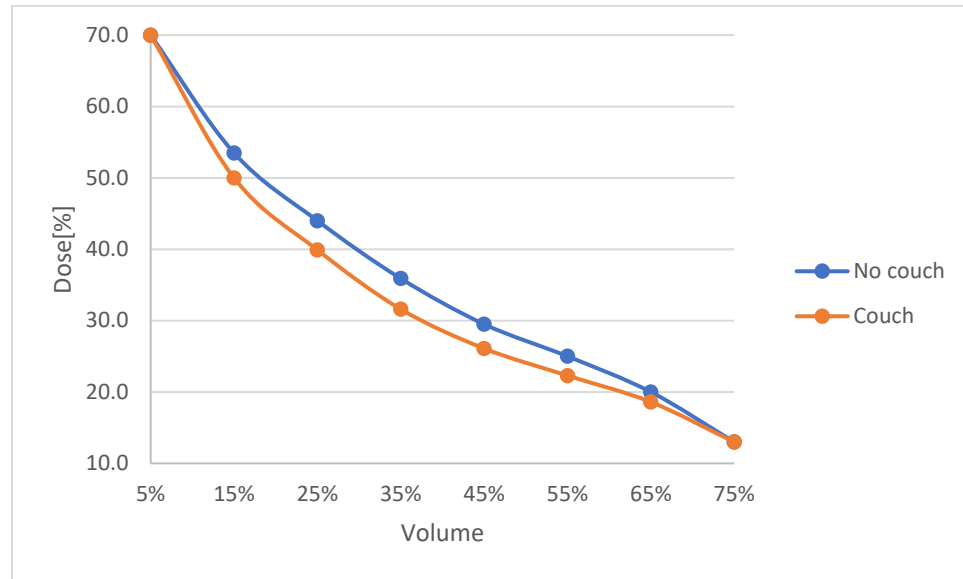


Figure 23: Does percentage distribution for left parotid gland between 75% and 5% of the volume

For the right brachial plexus, the mean dose dropped by 0.35 Gy. The dose differences between the two planes only exist between the doses covered from 85% to 70% of the volume.

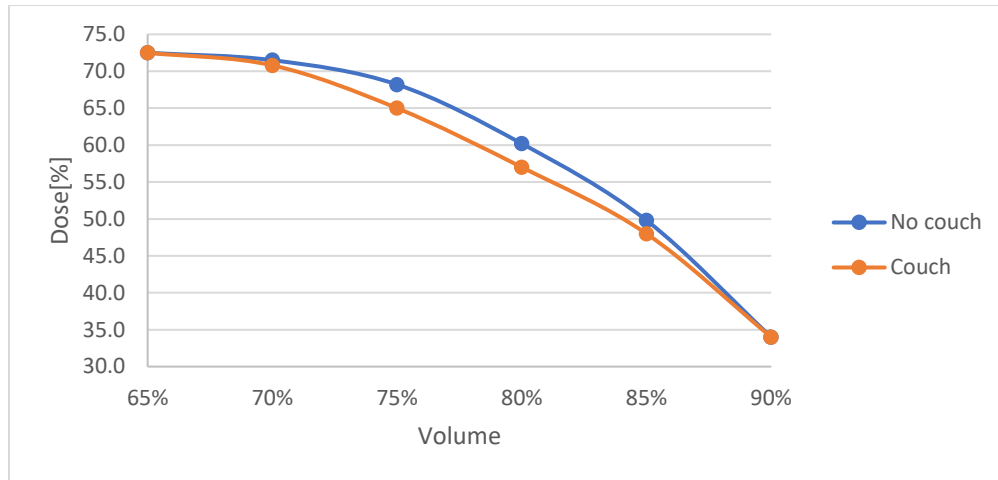


Figure 24: Does percentage distribution for right brachial plexus between 90% and 65% of the volume

For the left brachial plexus, the mean dose dropped by 0.21 Gy. The couch included plane has higher doses from 90% to 60% of the structure volume, however, the doses covered from 50% to 30% become higher for the couch excluded plane as shown in the figure below.

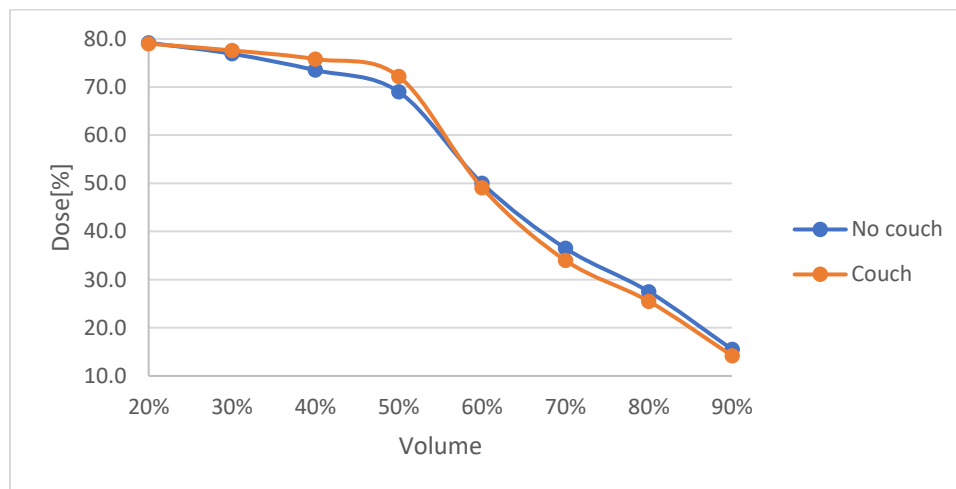


Figure 25: Does percentage distribution for left brachial plexus between 90% and 20% of the volume

#### 4.4 Summary of Dose Differences between Two Plans for All Patients.

<b>Target Structures</b>	<b>Patient 1</b>	<b>Patient 2</b>	<b>Patient 3</b>	<b>Patient 4</b>	<b>Average change</b>	<b>SD</b>
<b>PTV 70</b>	-0.5	-0.9	-0.9	-0.9	-0.8	0.2
<b>PTV 63</b>	-0.4	-0.9	-1.3	-1.1	-0.9	0.4
<b>PTV 56</b>	-0.4	-1.2	-0.7	-0.6	-0.7	0.3

Table 16: Mean dose change in the target structures for the all patients [% of 70 Gy]

<b>Normal structures</b>	<b>Patient 1</b>	<b>Patient 2</b>	<b>Patient 3</b>	<b>Patient 4</b>
<b>Spinal cord</b>	-0.6	0.3	-3.1	-2.8
<b>Mandible</b>	-0.3	-0.5	-0.7	0.1
<b>L Parotid</b>	-1.0	-0.0	-2.5	-2.0
<b>R Parotid</b>	-0.5	-0.1	-4.6	-0.5

Table 17: Mean dose changes for some normal structures [% of 70 Gy]

## **5.0 DISCUSSION**

Overall, the evaluation of the patient DVH data demonstrated a difference between dose modeling with the couch present as compared to when the couch was excluded. When the IGRT Couch Top® was included in the treatment planning system, there were losses of dose and coverage to target structures and dose differences to organs at risk. Findings indicate that when treatment planning considers the presence of the couch, modeling results reveal volumetric dose differences. In general, the goal of treatment planning is to be as accurate as possible, so that when unavoidable dose variations occur in actual treatment, they aren't added to planning errors.

### **5.1 Target Structures**

As mentioned previously in section 2.2.2, the prescription required irradiation of three targets: PTV 70, PTV 63, and PTV 56. The mean dose losses to the three target structures in all patients, on average, are 0.8%, 0.9%, and 0.7% for PTV 70, PTV 63, and PTV 56 respectively. The highest dose reduction of 1.3% for PTV 63 was seen in the third patient. However, both plans met the treatment criteria which were summarized in Table 1. The dose homogeneity for the PTV 70 was evaluated by calculating the homogeneity index (HI). The zero value indicates highly homogeneity in the dose distribution. The HI for the Couch excluded plan is  $0.08 \pm 0.02$  and for the Couch included plan is  $0.09 \pm 0.02$ . For two of the patients the HI was between 0.01 and 0.02 worse with the couch-included plan. For the other two patients, there was less difference.



## **5.2 Normal Structures**

For organs-at-risk, there was no consistent overall pattern to conclude any got less dose or more dose as a result of considering the couch in the treatment planning process. However, the TPS was able to achieve the dose constraints for the organs at risk for both plans as it was summarized in Table 2.

### **5.2.1 Spinal Cord**

Maximum doses dropped for three patients and the highest reduction of 7% was seen for the third patient. For the first patient, the maximum dose increased insignificantly with only 1%. The tolerance of the spinal cord to the radiation therapy is that the maximum dose should be less than 50 Gy to avoid the risk of the myelopathy.<sup>24</sup> This limit is not exceeded by any of the cases.

### **5.2.2 Mandible**

The dose differences for the mandible between two scenarios are evaluated for the first, second, and third patients, as dose differences were more easily observable from DVH plots. The maximum dose increases after the couch tops are included in TPS for those patients. The maximum difference of 2.3% is seen in the third patient. However, the mean dose decreases for the Couch included plans.

### **5.2.3 Larynx**

The maximum and mean dose increase for the first patient as the couch inserted in TPS. However, for the third and fourth patients, these doses are dropped. The highest dose reduction was found to be 4.3% is seen in the third patient.

#### **5.2.4 Right and Left Parotid Gland**

In the couch included planes, the maximum and mean doses are dropped and the highest difference of 5.2% is seen in the third patient. However, the maximum dose of the left parotid gland is out of the norm and increases as the couch top considered on the plane.

## 6.0 CONCLUSION

In this study, the effects of the Varian IGRT Couch Top<sup>®</sup> on the dose distribution of the head and neck cancers treatment was determined for a linear accelerator operating at 6 MV. Four head and neck cancer patient plans were randomly selected for the study. Plans were conducted both with and without couch insertion, where the change in dose distribution and volumetric dose statistics in a Varian Model Eclipse<sup>®</sup> treatment planning system would give rise to the consequence of the couch being modeled in the beam. Comparisons were made using the planning system's Dose Volume Histogram (DVH). Regarding dose to PTV, both plans achieved the physicians' dose criteria for all four patients. However, there was a trend with the couch-included plans that the dose barely achieved the clinical criteria. For example, the criteria for PTV 70 was  $D_{99} = 97\%$ . The four couch excluded plans achieved 99%, 99%, 101%, and 99%, and the four couch included plans achieved 98%, 98%, 100%, and 98%. For organs-at-risk, there was no consistent overall pattern to conclude any got less dose or more dose as a result of considering the couch in the treatment planning process. The results of this work indicate that while the treatment couch may make achieving the physician's criteria more difficult, the treatment planning software was able to develop an acceptable plan in all cases.

## REFERENCES

- <sup>1</sup>Ost, Bie De, et al. “The effect of carbon fibre inserts on the build-up and attenuation of high energy photon beams.” *Radiotherapy and Oncology* 45(3), 1997, pp. 275–277
- <sup>2</sup> S. J. Meara, and A. K. Langmack. “An investigation into the use of carbon fibre for megavoltage radiotherapy applications.” *Physics in Medicine and Biology* 43(5), 1998, pp. 1359–1366
- <sup>3</sup> S. McCormack, et al. “The effect of gantry angle on megavoltage photon beam attenuation by a carbon fiber couch insert.” *Medical Physics* 32(2), 2005, pp. 483–487
- <sup>4</sup> C. Njeh, T. Raines, and M. Saunders “Determination of the photon beam attenuation by the BrainLAB imaging couch: angular and field size dependence.” *Journal of Applied Clinical Medical Physics* 12(1), 2009, pp. 241–241
- <sup>5</sup> J. K. H. Seppälä, and J. A. J. Kulmala, “Increased beam attenuation and surface dose by different couch inserts of treatment tables used in megavoltage radiotherapy,” *Journal of Applied Clinical Medical Physics* 12(4), (2011), pp. 15
- <sup>6</sup> S. Vieira, et al. “Two-Dimensional measurement of photon beam attenuation by the treatment couch and immobilization devices using an electronic portal imaging device.” *Medical Physics*, 30(11), 2003, pp. 2981–2987
- <sup>7</sup> R. K. Munjal, et al. “Impact of 6MV photon beam attenuation by carbon fiber couch and immobilization devices in IMRT planning and dose delivery,” *Journal of Applied Clinical Medical Physics* 31(2), (2006), pp. 67
- <sup>8</sup> K. R. Pulliam, et al. “The clinical impact of the couch top and rails on IMRT and arc therapy,” *Physics in Medicine and Biology* 56, (2011), pp. 7435-7447
- <sup>9</sup> W. K. Myint, et al. “Investigating treatment dose error due to beam attenuation by a carbon fiber tabletop.” *Journal of Applied Clinical Medical Physics*, vol. 7, no. 3, 2006, pp. 21–27
- <sup>10</sup> Z. Hu, J. Dai, L. Li, Y. Cao, and G. Fu, “Evaluating and modeling of photon beam attenuation by a standard treatment couch,” *Journal of Applied Clinical Medical Physics* 12(4), (2011), pp. 139

- <sup>11</sup> L. H. Gerig, M. Niedbala, and, B. Nyiri, “Dose perturbations by two carbon fiber treatment couches and the ability of a commercial treatment planning system to predict these effects,” *Medical Physics* 37, (2010), pp. 32
- <sup>12</sup> I. B. Mihaylov, P. Corry, Y. Yan, V. Ratanatharathorn, and, E. G. Moros, “Modeling of carbon fiber couch attenuation properties with a commercial treatment planning system,” *Medical Physics* 35, (2008), pp. 4982
- <sup>13</sup> Vanetti, E., et al. “The Impact of treatment couch modeling on RapidArc.” *Physics in Medicine and Biology* 54, (2009), pp. 157-166
- <sup>14</sup> F. M. Kahn, *The Physics of Radiation Therapy*, 4th ed. (Lippincott Williams & Wilkins, Philadelphia, PA, 2010).
- <sup>15</sup> E. B. Podgorsak and J. H. Hendry, *Radiation Oncology Physics: A Handbook for Teachers and Students* (International Atomic Energy Association, Vienna, 2005).
- <sup>16</sup> J. Bushberg, J. Seibert, E. Leidholdt Jr., and J. Boone, *The Essential Physics of Diagnostic Radiology*, 4th ed. (Lippincott Williams and Wilkins, Philadelphia, PA, 2001).
- <sup>17</sup> J. E. Turner, *Atoms, Radiation, and Radiation Protection*, 3rd ed. (Wiley-VCH, Berlin, Germany, 2007).
- <sup>18</sup> S. Forshier, *Essentials of radiation biology and protection*, 2nd ed. (Delmar, Clifton Park, NY, 2009).
- <sup>19</sup> W. Kalender. *Computed tomography: fundamentals, system technology, image quality, applications*. MCD Verlag, 2000.
- <sup>20</sup> International Commission on Radiation Units and Measurements, “Prescribing, recording, and reporting photon beam therapy”, ICRU Report 50 (1993).
- <sup>21</sup> International Commission on Radiation Units and Measurements, “Prescribing, recording, and reporting photon-beam intensity- modulated radiation therapy (IMRT)”, ICRU Report 83 (2010).
- <sup>22</sup> Hubbell, J H. “Tables of x-Ray mass attenuation coefficients and mass energy-Absorption coefficients 1 keV to 20 MeV for elements  $Z = 1$  to 92 and 48 additional substances of dosimetry interest.” 1995.

<sup>23</sup> Minus, M, and S Kumar. “The processing, properties, and structure of carbon fibers.” JOM 57(2), 2005, pp. 52–58.

<sup>24</sup> Emami, B., et al. “Tolerance of normal tissue to therapeutic irradiation.” International Journal of Radiation Oncology Biology Physics 21(1), 1991, pp. 109–122.